ACS Photonics

Article

pubs.acs.org/journal/apchd5

Efficient Energy Transfer between Si Nanostructures and Er Located at a Controlled Distance

Halina Krzyżanowska,*[,†,‡] Yijing Fu,[§,∥] Karl S. Ni,[⊥,#] and Philippe M. Fauchet[⊥,○]

[†]Department of Physics and Astronomy and [○]Department of Electrical Engineering and Computer Science, Vanderbilt University, Nashville, Tennessee 37235, United States

[‡]Maria Curie-Sklodowska University, Pl. M. Curie-Sklodowskiej 1, 20-031 Lublin, Poland

[§]The Institute of Optics and [⊥]Department of Electrical and Computer Engineering, University of Rochester, Rochester, New York 14627, United States

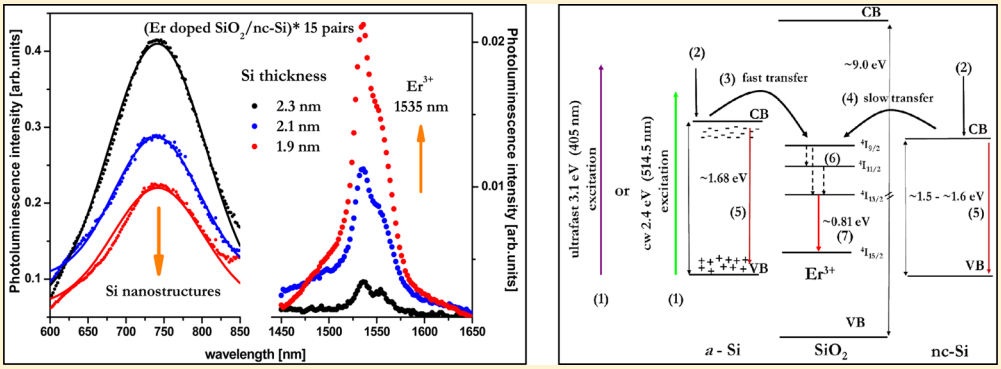

ABSTRACT: Systematic studies of the relaxation processes in nm-thick Er-doped SiO_2/nc-Si multilayers have been conducted using cw photoluminescence and time-resolved photoluminescence. The size of the Si nanocrystals is determined by thickness of the Si layer. The distance between the Si nanocrystals and the Er ions in the SiO_2 layers is fixed between 0 and 2.2 nm. An efficient energy transfer from amorphous and crystalline Si nanostructures to Er is observed and leads to a strong Er photoluminescence at 1535 nm, which increases as the Si layer thickness decreases. The fast Er photoluminescence (μs lifetime) results from energy transfer from *a*-Si nanostructures and the slow Er emission (ms lifetime) is caused by energy transfer from confined states in nc-Si. The transfer time was estimated to be 20 ± 5 ns by a direct time-resolved photoluminescence experiment. A model is proposed to explain these results.

KEYWORDS: *Er-doped SiO_2/Si multilayers, Si nanostructures, 1535 nm Er emission, energy transfer, time-resolved photoluminescence, silicon photonics*

The element Er and its oxides play a very important role as an active material for optoelectronic applications, such as sources based on Er-doped silicon structures. Some of the candidates to attain this goal include different types of materials such as Er:Si/Si,[1] Er:Si-rich SiO_2/SiO_2,[2] Er:SiO/SiO_2,[3] Er:SiN/Si,[4] Si, or SiO_2 layers doped with Er by implantation,[5] or Er and ErY silicates fabricated by RF magnetron sputtering.[6,7] Recently, we reported on efficient photo- and electroluminescence from Er-doped SiO_2/nc-Si multilayers.[8,9] Despite an impressive amount of this research, the efficiency of these light sources remains low.

Here, we report cw photoluminescence (PL) studies and time-resolved (TR) PL measurements. Previous studies on Er doped nc-Si/SiO_2 superlattices have shown neither strong room temperature luminescence of the Si nanocrystals nor efficient Er^{3+} emission at 1535 nm.[10] The multilayers examined here are different from the samples described in earlier studies[1−7] in several aspects. The Si nanocrystals are located in well-defined planes as they are formed by annealing of thin amorphous Si (*a*-Si) layers.[11−13] The thickness of the *a*-Si layers determines the nanocrystal size and thus the characteristics of the Si-related emission in the 740−800 nm spectral window. The maximum distance between any Si nanocrystal and any Er ion is 2.2 nm, which is half of the thickness of the SiO_2 layers or less.

When Er is incorporated into the SiO_2 layers, the Si-related PL intensity decreases and the 1535 nm Er-linked PL intensity increases as a result of energy transfer from the photoexcited Si nanocrystals and amorphous Si nanostructures to Er. The nature of the energy transfer in Er doped structures is still a matter of some uncertainty.[14,15] Dexter energy transfer and Förster energy transfer from nc-Si to Er ions are the two possible mechanisms.[4,14,15] The most crucial parameter in these processes is the distance between the Si nanocrystals and the Er located in the adjacent SiO_2 layers. Our multilayer structures

Received: September 11, 2015
Published: March 3, 2016

DOI: 10.1021/acsphotonics.5b00515
ACS Photonics 2016, 3, 564−570

offer two advantages: the size of the Si nanostructures is tightly controlled and the distance between the nc-Si and the Er ions can be quantified.[10−12]

In this work, we present strong, room temperature Er photoluminescence at 1535 nm from Er-doped SiO_2/nc-Si multilayers and discusses its origin via the analysis of the visible and infrared PL lifetimes. Two PL decay times (fast and slow) are identified both at 740 nm from Si nanostructures and at 1535 nm from Er. We interpret the fast Er photoluminescence (μs lifetime) as due to energy transfer from *a*-Si nanostructures and the slow Er emission (ms lifetime) as caused by energy transfer from confined states in nc-Si. The energy transfer time from Si nanostructures to Er in SiO_2 is measured, in a direct experiment, to be 20 ± 5 ns.

EXPERIMENTAL SECTION

Multilayer samples were prepared using a multigun (Si, SiO_2, Er) magnetron sputtering system (ATC 2200, AJA International). Reference SiO_2/nc-Si (no Er) and Er-doped SiO_2/nc-Si multilayers were prepared. The multilayers were produced by the sequential deposition of layers of amorphous silicon and layers of SiO_2 cosputtered with Er on a Si(100) substrate. The Er concentration measured by Secondary Ion Mass Spectrometry was estimated to be 2×10^{20} atoms/cm^3. Crystallization of the *a*-Si layers was achieved by furnace annealing at 1050 °C in Ar for 1 h.[9,11,12,16] The thickness of the individual *a*-Si layers was 1.9, 2.1, and 2.3 nm, and that of the SiO_2 layers was fixed at 4.5 nm. The accuracy of the average thickness was estimated to be ±3.6% and ±2.5% for the Si and SiO_2 layers, respectively, using the deposition rates for Si and SiO_2 layers determined from spectroscopic ellipsometry[9] as well as from TEM pictures and the deviation of the layer uniformity from the manufacture web site.[17] Figure 1 presents a sketch of the structures under

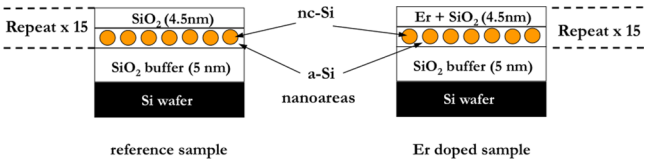

Figure 1. Schematic view of the studied multilayers: reference (left) and Er-doped (right). The SiO_2 thickness is fixed at 4.5 nm.

study. Note that at these thicknesses, the conversion from *a*-Si into nc-Si is not complete and some *a*-Si remains in the Si layers after annealing.[12,13,16,18] A representative TEM picture of the SiO_2/nc-Si multilayer structure was shown in our earlier works.[8,16]

The spectral resolution in all PL measurements was assessed as ∼5 nm (1/4 m Oriel monochromator 257). Cw photoluminescence spectra were carried out at room temperature using the Ar^+ laser line at 514.5 nm, which is off resonance with Er^{3+}.[19,20] PL spectra were recorded at room temperature using photomultipliers tubes (Hamamatsu R2066 for the visible region and thermoelectrically cooled Hamamatsu H10330B-75 for the infrared region). The time-correlated photon-counting technique (TimeHarp200, PicoQuant) was used to collect the time-resolved PL after 405 nm excitation with femtosecond laser pulses from a frequency-doubled Ti:sapphire laser system with a 200 Hz repetition rate. The time resolution of these measurements was estimated to be 0.5 ns.

RESULTS

Photoluminescence spectra from a reference and an Er doped SiO_2/nc-Si multilayer are presented in Figures 2 and 3. In the spectra from the Er-free (reference) samples, the broad PL spectra, centered at ∼780 nm blue shifts as the Si layer thickness decreases (Figure 2). This result is in general agreement with the PL maxima shift reported earlier.[5,21,22] Such broad PL is the outcome of emission from Si nanocrystallites, from the embedding *a*-Si matrix and from the interface between the two as well.[23] Deconvolution of these spectra was done with two Gaussian distributions with a maximum at ∼740 nm linked to *a*-Si[24,25] and another maximum that varied from ∼780 to ∼800 nm, depending on the nc-Si size from 1.9 to 2.3 nm (Figure 2). Note the total photoluminescence signal from *a*-Si nanostructures is very similar for both sizes: the difference in intensity for samples with Si layers of 1.9 and 2.3 nm is less than 5%. Theory shows that the *a*-Si energy gap increases significantly only for slabs thinner than 1.2 nm. For *a*-Si slabs with thicknesses between 1.9−2.3 nm, the change of energy gap was calculated to be 0.01−0.03 eV.[24,26,27] Since the localization length of carriers in *a*-Si, estimated to be 0.6−1 nm,[28−30] is less than the *a*-Si thickness, no quantum confinement effects on the PL peak energy are expected for our structures. From the nc-Si structures, the total PL intensity increases with decreasing nc-Si size, as expected from theory[31] (Figure 2).

In contrast, when the SiO_2 layers are doped with Er, the PL spectra show no measurable blue shift when the thickness of the Si layer decreases. The peak at ∼740 nm, characteristic for amorphous Si nanostructures[24,25] (Figure 3). We attribute the PL as a result of transitions between strongly localized states in *a*-Si.[24−26]

More importantly, unlike the reference spectra, the thinnest Si layer (1.9 nm) yields the weakest ∼740 nm PL intensity and the strongest Er-related infrared PL intensity at 1535 nm (see Figure 3). The simultaneous increase in Er-related PL and decrease in PL from Si nanostructures demonstrates direct evidence of energy transfer from Si nanostructures to Er in the adjacent SiO_2 layers.

Time-resolved photoluminescence (TR PL) collected at 740 nm from both reference and Er-doped multilayers is shown in Figure 4a as a function of the Si layer thickness. The PL decay spectra are the results of radiative and nonradiative transitions in amorphous and nanocrystalline components. All spectra have been fitted as the sum of two exponentials:

$$I = I_{\text{fast}} \exp(-t/\tau_{\text{fast}}) + I_{\text{slow}} \exp(-t/\tau_{\text{slow}}) \quad (1)$$

known in the literature as the "fast" and "slow" PL decay channels.[14,32] Figure 4b,c show the fast and slow lifetimes as a function of the Si layer thickness, which determines the nanocrystal diameter. No Si nanocrystal size (layer thickness) dependence is observed in the reference samples, whereas both lifetimes decrease rapidly with decreasing nc-Si size in the Er-doped specimens (see Figures 4b,c).

For the reference samples the fast and slow decay times are 3.7 and 34 μs, respectively. These values are in a good agreement with the lifetimes observed from *a*-Si (of the order of few μs) and from radiative transitions in nc-Si (tens of μs).[32−35] Hence, we attribute the fast lifetime to *a*-Si nanostructures and the slow decay to nc-Si.

In the case of Er doped multilayers, both fast and slow lifetimes of the visible (740 nm) TR PL spectra are faster than those from the reference samples (Figure 4b,c). The values of

DOI: 10.1021/acsphotonics.5b00515
ACS Photonics 2016, 3, 564−570

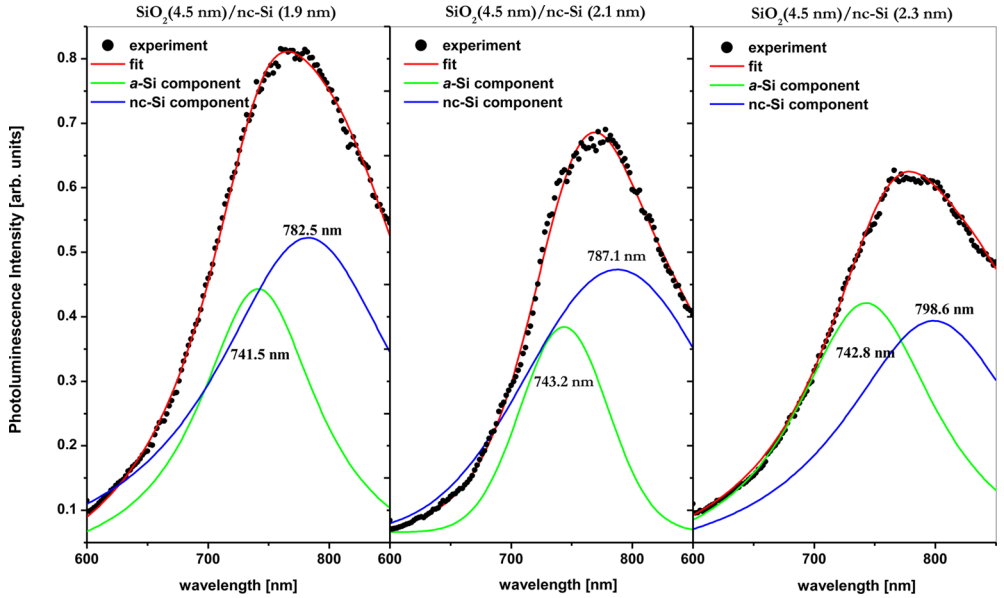

Figure 2. Room temperature visible photoluminescence spectra excited at 514.5 nm from three reference samples with and Si layers of 1.9, 2.1, and 2.3 nm and identical SiO_2 layer of 4.5 nm. The solid lines represent Gaussian fits. The PL intensity is not normalized and corresponds to the same arbitrary unit in all figures.

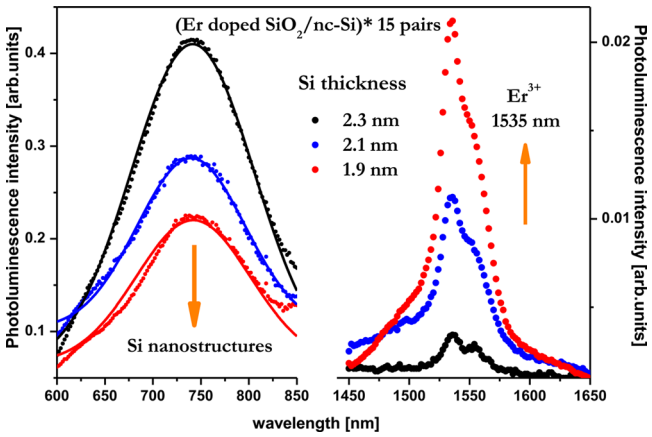

Figure 3. Room temperature visible and infrared PL spectra from Er-doped multilayers with different Si layer thicknesses excited at 514.5 nm. The solid lines represent Gaussian fits. The VIS PL intensity is not normalized and corresponds to the same arbitrary unit as in Figure 2.

τ_{fast} and τ_{slow} and their dependence of nc-Si size are strikingly different compared to the reference samples. The fast decay time decreases from 3.6 to 1.7 μs and the slow decay time also decreases from 33 to 19 μs as the Si thickness decreases from 2.3 to 1.9 nm. This result in combination with the observation that a weaker visible cw PL is associated with a stronger Er emission reflects an additional nonradiative process present in the Er-doped multilayers. The most likely decay pathway is via transfer of energy from Si nanostructures (donor) to Er (activator). Additionally, the amplitude of the fast lifetime (due to *a*-Si) is approximately 40× stronger than that of the slow lifetime (due to nc-Si). This fact confirms the cw PL results where no noticeable contribution from nc-Si was observed (see Figure 3).

To complete our studies and to monitor the Er luminescence, infrared PL was collected at 1535 nm. Under 405 nm excitation, there is no PL signal detected at 1535 nm from the reference sample while a strong response from the Er doped structure is observed (Figure 5a). Figure 5b presents TR PL spectra for two different Si layer thicknesses. The intensity of the Er luminescence is higher for the smallest Si nanocrystals, consistent with Figure 3. The decay consists of a fast initial decrease followed by an approximately exponential tail with a characteristic Er^{3+} decay time of the order of microseconds. A biexponential fit was also used to determine the IR PL lifetimes. The fast lifetimes at 1535 nm for the multilayers with 1.9 and 2.3 nm Si thickness were estimated as 24.6 and 29.4 μs, respectively (Figure 5b). This fast PL can be associated with indirectly excited Er^{3+} transitions.[14] We link this emission to excitation via energy transfer from *a*-Si nanostructures. The slow IR decay time for both multilayers was estimated of the order of 3 ms, which is typical for Er^{3+} in a SiO_2 matrix.[7,15,35−37]

TR PL spectra in the time window of 130 ns are shown in Figure 5c. The spike near $t = 0$ in the Er-free (references) sample is the result of scattered light from the excitation beam. The rise time of the Er-doped spectrum, obtained after subtraction of the scattered light peak, is 20 ± 5 ns, which corresponds directly to the energy transfer time (in blue, Figure 5c). This time covers transfers from both amorphous and crystalline Si nanostructures. The time resolution in our experiment (±0.5 ns) and the noise in the data does not allow us to separate the transfer time of these two components. We observe no significant changes of the estimated transfer time for other Er-doped samples (Figure 5d).

DISCUSSION

Extensive studies of energy transfer mechanism in Er-doped, silicon-rich, SiO_2 films prepared by sputtering have been reported by Savchyn et al.,[38] Izeddin et al.,[35,37] and Pitanti et al.[15] In these studies, Si nanocrystals were formed during annealing from excess Si atoms in a SiO_2 matrix.[15,35,37,38]

Savchyn et al.[38] indicate that discrete luminescence centers (LCs) associated with excess-silicon related electronic defects in SiO_2 matrix are responsible for most of the indirect Er^{3+} excitation for all annealing temperatures, with a small

DOI: 10.1021/acsphotonics.5b00515
ACS Photonics 2016, 3, 564−570

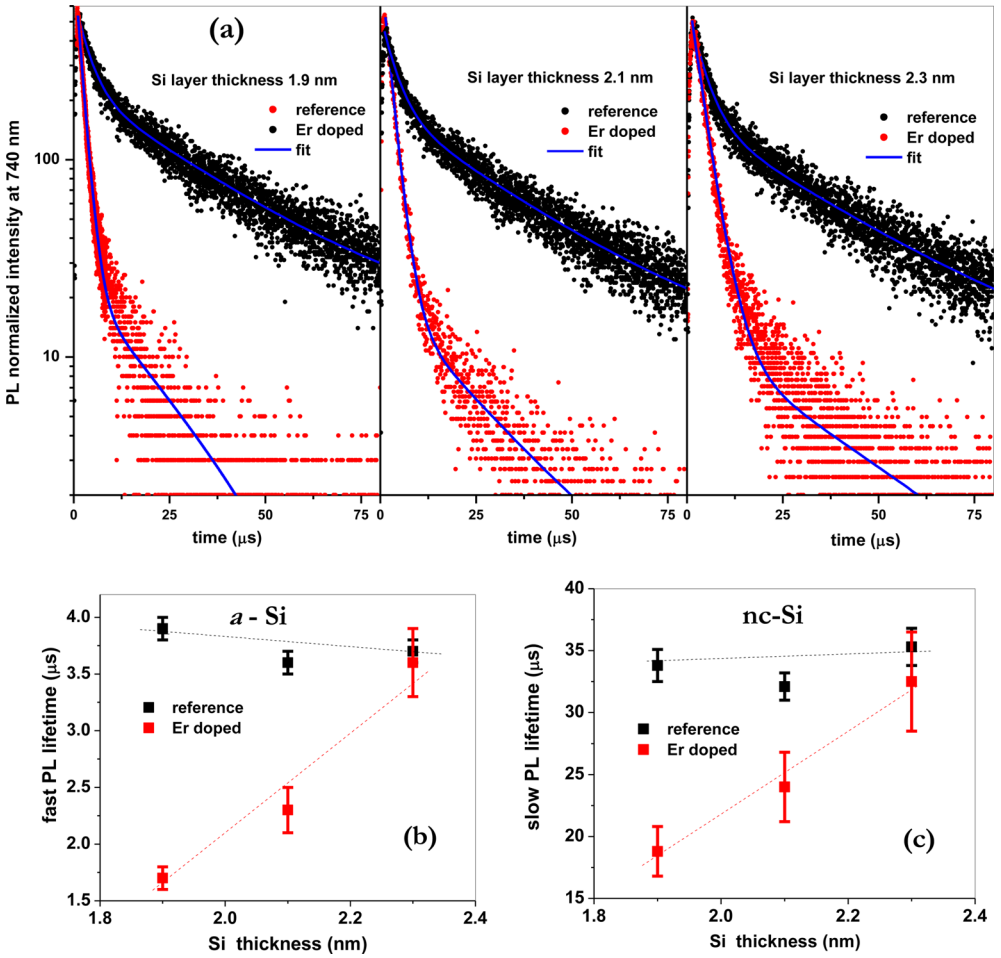

Figure 4. (a) Sequence of time-resolved visible PL dynamics from reference and Er-doped multilayers. The blue lines represent biexponential fits as discussed in the text. (b) Fast and (c) slow PL lifetimes at 740 nm from the reference and Er-doped multilayers vs Si layer thickness. The dashed lines in (b) and (c) are a guide to the eye. All fits for the visible PL data was done using eq 1 and Matlab code with Levenberg−Marquardt nonlinear regression.[45] The uncertainty of the lifetimes was calculated from the diagonals of the covariance matrix.[45]

contribution due to Si nanocrystals formed at higher annealing temperatures (>1000 °C). Si nanocrystals of various sizes and Er ions are randomly distributed in the SiO_2 matrix. Thus, the distance between nc-Si and Er, which determines the efficiency of the energy transfer, cannot be established precisely. There is no indication of amorphous Si phase in this system. These authors identify two distinct transfer times: fast (<80 ns) attributed to the Er^{3+} excitation via only LCs and slow (4−100 μs) due to the energy transfer mediated by emission from excited nc-Si. In our samples, the nanocrystal diameter is precisely controlled by the thickness of the *a*-Si layers, and there is no single Si atoms dissolved in the SiO_2 matrix that could serve as LCs.

Izeddin et al.[35,37] discuss temporal details of emission bands from Er^{3+} and nc-Si located in an SiO_2 matrix. The PL spectrum from a reference sample shows two maxima. The first maximum at 775 nm is not sensitive to the nc-Si size and is attributed to recombination of carriers from higher electronic states in nc-Si. The peak of the second band near 850 nm depends on the nc-Si size and is attributed to excitonic PL in nc-Si. The decay time of this band, for a sample with an average nc-Si diameter of 3.1 nm was estimated as 20−50 μs.[35] Their decay time is in very good agreement with that obtained from our reference multilayers. The time-resolved PL near 1.5 μm exhibits three regimes in the Er kinetics, which are explained as follows by these authors: a fast decay (<1 μs) caused by a fast energy transfer involving cooling of hot carriers via an Auger process and direct excitation of Er^{3+} ions to the first $^4I_{13/2}$ energy level, a slow rise (1−10 μs) associated with the slow energy transfer between nc-Si and Er, and a slow decay (>10 μs) where Er^{3+} ions are excited via intraband transition of confined carriers in nc-Si.

In contrast to the Er kinetics discussed in refs 35 and 37, we observe a double exponential Er PL decay and describe the fast PL (Er μs lifetime) as due to transfer from *a*-Si nanostructures and the slow PL (Er ms lifetime) as resulting from energy transfer from confined states in nc-Si.

In the report by Pitanti et al.,[15] the transfer time for the 980 nm Er emission line in the Si-rich SiO_2 system implanted with Er was estimated to be 36 ± 10 and 117 ± 30 ns for the case of *a*-Si nanoparticles and nc-Si, respectively. Our measured transfer time of 20 ns in the multilayers studied averages both *a*-Si nanostructures and nc-Si components. This time is much faster than that for the implanted samples with emission at 980 nm.[15] Although the authors of ref 15 have also studied the 1535 nm Er emission by TR PL, they do not report the transfer time for this important Er emission wavelength.

To follow the origin of the Er strong luminescence from our samples, a model of energy transfer in the Er-doped multilayers is proposed in Figure 6. We consider cw excitation at 2.4 eV

DOI: 10.1021/acsphotonics.5b00515
ACS Photonics 2016, 3, 564−570

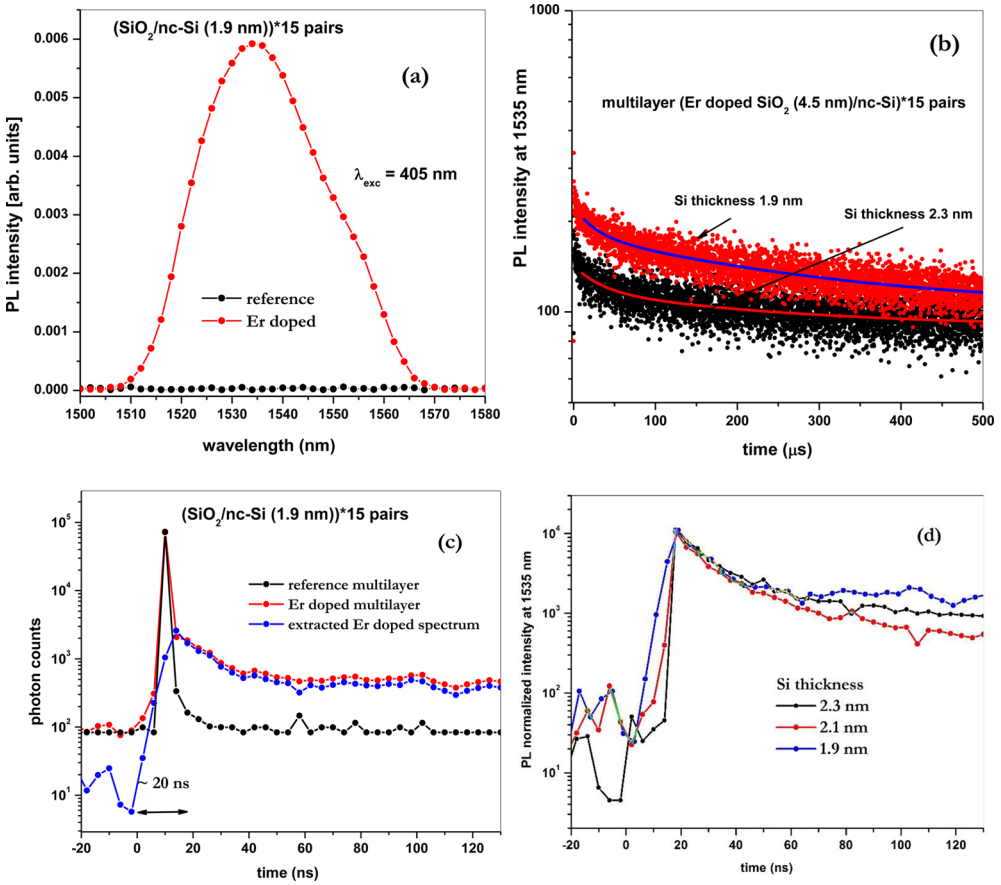

Figure 5. IR PL spectra from reference and Er-doped multilayers; (a) PL spectrum under pulsed 405 nm excitation. A 1535 nm line is observed from Er-doped structure. No PL signal was detected for the reference multilayer; (b) Time-resolved decays for Er-doped multilayers with 1.9 and 2.3 nm Si layer thicknesses revealing two decay times. The lines represent biexponential fits; (c) Normalized time-resolved PL spectra of the reference (black) and Er-doped (red) in the 150 ns temporal window. The extracted Er-doped spectrum (blue) was obtained by subtraction the Er-doped data from the reference data. It clearly shows the rise time estimated to be about 20 ns and is directly related to the time of energy transfer from Si nanostructures to Er. (d) Normalized extracted Er-doped spectra for different Si layer thicknesses.

and femtosecond pulsed excitation at 3.1 eV (process (1) in the Figure 6). The excited hot carriers relax very rapidly to the lowest energy states in the conduction and valence bands of *a*-Si and nc-Si structures (process (2) in Figure 6). In *a*-Si, the excited carriers thermalize down through the localized band tail states by phonon-assisted transitions.[24,39,40]

Energy transfer occurs from both types of Si nanostructures (processes (3) and (4) in Figure 6). The cw PL spectra (Figure 3) and the TR PL decay spectra at 740 nm (Figure 4a) from Er-doped samples reflect recombination of carriers to the ground state of *a*-Si mostly via radiative transitions and to the ground state of nc-Si mostly via non- radiative processes (process (5) in Figure 6). Finally, the Er emission at 1535 nm is observed (process (7) in Figure 6) as a result of the efficient Er energy transfer.

The distance between Si and Er atoms is the key parameter in determining the efficiency of the energy transfer.[14,15] For the Dexter energy transfer mechanism, the distance between the sensitizer (nc-Si) and the activator (Er atom) needs to be 0−1 nm,[41] while for the Förster mechanism it can range from 0−10 nm.[42]

In our samples, assuming a homogeneous Er distribution in the SiO_2 layers, there is approximately one Er ion less than 2.2 nm (i.e., half of the SiO_2 thickness) away from each Si nanocrystal in the SiO_2 layers above and below. Nearly 50% of the Er atoms are so close (≤1 nm) to the nc-Si that overlap of the wave functions can occur, allowing Dexter energy transfer. Note that it has been shown in thicker Er-doped SiO_2 structures (50 nm) cladded by Si layers[43] that the Er concentration is inhomogeneous after annealing and that Er atoms move toward the SiO_2/Si interface. If this is the case in our structures too, a higher concentration of Er near the nc-Si makes the Dexter process even more likely. As the nc-Si diameter increases, the electron and hole wave functions extend less in the SiO_2 and the Dexter process becomes less dominant. In all our multilayers the distance between nc-Si and Er ions covers the Förster energy transfer distance requirement between the sensitizer and the activator. If this process was responsible for the efficient Er emission at 1535 nm, no significant reduction of infrared PL should be observed with an increase of the Si nanocrystal size. From these considerations, we conclude that PL emission at 1535 nm occurs mainly due to the Dexter process. Our measured transfer time of 20 ns agrees well with theory.[41]

CONCLUSION

In this paper, we demonstrated strong emission at 1535 nm from Er doped SiO_2/nc-Si multilayers under Er off-resonant excitation and discussed the relaxation dynamic of the visible and IR photoluminescence. Systematic studies of reference (SiO_2/nc-Si) and Er-doped SiO_2/nc-Si multilayers revealed that

DOI: 10.1021/acsphotonics.5b00515
ACS Photonics 2016, 3, 564−570

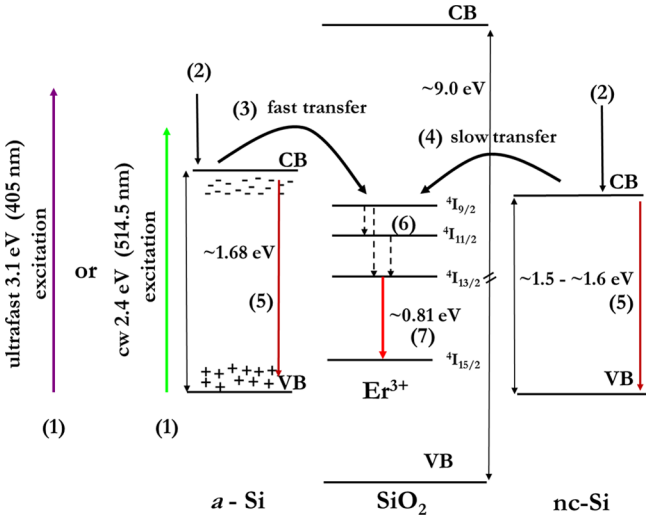

Figure 6. Simplified (not in scale) energy band diagram for the proposed kinetics of the PL process in Er-doped SiO_2/nc-Si multilayers; (1) excitation by ultrafast or cw laser; (2) very fast thermalization of hot carriers to the band tails; (3) fast energy transfer from *a*-Si nanostructures to Er^{3+}; (4) slow energy transfer from nc-Si to Er^{3+}; (5) radiative recombination processes (photoluminescence) in *a*-Si nanostructures and in nc-Si-competitive processes to the energy transfer; (6) exemplary nonradiative transitions from higher excited states to $^4I_{13/2}$ in Er^{3+} located in SiO_2 matrix; (7) infrared luminescence from Er^{3+} at 1535 nm; symbols "−" and "+" in *a*-Si represent localized states; VB, valence band; CB, conduction band.

the fast and efficient Er emission at 1535 nm is due to effective energy transfer. The reduction in visible PL intensity and shortening of the visible PL lifetime for the Er doped samples are due to the energy transfer from Si nanostructures to Er ions. The key parameter in the transfer process, the distance between Si nanostructures and Er, is well controlled in our system. The fast (μs) Er lifetime is due to the transfer from *a*-Si nanostructures and the slow (ms) Er lifetime is caused by the energy transfer from confined states in nc-Si. The transfer process involves both nc-Si and *a*-Si nanostructures and results in fast and efficient indirect Er exitation. The transfer time was estimated to ~20 ns and is faster for 1535 nm than for 980 nm.[15]

The combination of having a short controllable distance between Er and Si nanostructures, one Er ion less than 2.2 nm away from each Si nanocrystal in the SiO_2 layers above and below, and confinement of light inside the SiO_2 layers in a waveguide configuration[44] leads to effective energy transfer and elimination of free carrier absorption in Si nanocrystals,[18] both of which are required for efficient Si-based light amplifiers and lasers.

AUTHOR INFORMATION

Corresponding Author

*E-mail: halina.t.krzyzanowska@vanderbilt.edu.

Present Addresses

[‖]Microsoft Corporation, 15916 NE 42nd St., Redmond, WA 98052 (Y.F.).

[#]Quintel USA, Inc., 1200 Ridgeway Ave., Rochester, NY 14615 (K.S.N.).

Notes

The authors declare no competing financial interest.

ACKNOWLEDGMENTS

This work is supported by a MURI grant (FA9550-06-1-0344, G.P.). The authors thank R. S. Knox for many valuable discussions. H.K. thanks the Tolk group members for their assistance and conversations. H.K. acknowledges the Polish Ministry of Science and Higher Education for financial support under Grant 224/MOB/2008/0 and the ARO agency for the support under Contract No. W911NF-14-1-0290.

REFERENCES

(1) Vinh, N. Q.; Minissale, S.; Vrielinck, H.; Gregorkiewicz, T. Concentration of Er^{3+} Ions Contributing to 1.5-μm Emission in Si Si:Er Nanolayers. *Phys. Rev. B: Condens. Matter Mater. Phys.* **2007**, *76*, 085339.

(2) Gourbilleau, F.; Madelon, R.; Dufour, C.; Rizk, R. Fabrication and Optical Properties of Er-doped Multilayers Si-rich SiO_2/SiO_2: Size Control, Optimum Er-Si Coupling and Interaction Distance Monitoring. *Opt. Mater.* **2005**, *27*, 868−875.

(3) Adeola, G. W.; Jambois, O.; Miska, P.; Rinnert, H.; Vergnat, M. Luminescence Efficiency at 1.5 μm of Er-Doped Thick SiO Layers and Er-Doped SiO/SiO_2 Multilayers. *Appl. Phys. Lett.* **2006**, *89*, 101920.

(4) Dal Negro, L.; Li, R.; Warga, J.; Basu, S. N. Sensitized Erbium Emission from Silicon-rich Nitride /Silicon Superlattice Structures. *Appl. Phys. Lett.* **2008**, *92*, 181105.

(5) Timoshenko, V. Y.; Lisachenko, M. G.; Shalygina, O. A.; Kamenev, B. V.; Zhigunov, D. M.; Teterukov, S. A.; Kashkarov, P. K.; Heitmann, J.; Schmidt, M.; Zacharias, M. Comparative Study of Photoluminescence of Undoped and Erbium-Doped Size-Controlled Nanocrystalline Si/SiO_2 Multilayered Structures. *J. Appl. Phys.* **2004**, *96*, 2254−2260.

(6) Miritello, M.; Savio, R.; Lo; Iacona, F.; Franzò, G.; Irrera, A.; Piro, A. M.; Bongiorno, C.; Priolo, F. Efficient Luminescence and Energy Transfer in Erbium Silicate Thin Films. *Adv. Mater.* **2007**, *19*, 1582−1588.

(7) Miritello, M.; Lo Savio, R.; Cardile, P.; Priolo, F. Enhanced Down Conversion of Photons Emitted by Photoexcited $Er_xY_{2-x}Si_2O_7$ Films Grown on Silicon. *Phys. Rev. B: Condens. Matter Mater. Phys.* **2010**, *81*, 041411.

(8) Krzyzanowska, H.; Ni, K. S.; Fu, Y.; Fauchet, P. M. Electroluminescence from Er-doped SiO_2/nc-Si Multilayers under Lateral Carrier Injection. *Mater. Sci. Eng., B* **2012**, *177*, 1547−1550.

(9) Ni, K. S.; Krzyzanowska, H.; Fu, Y.; Fauchet, P. M. U.S. Patent 2014/0027808 A1, 2014.

(10) Schmidt, M.; Heitmann, J.; Scholz, R.; Zacharias, M. Bright Luminescence from Erbium-doped nc-Si/SiO_2 Superlattices. *J. Non-Cryst. Solids* **2002**, *299-302*, 678−682.

(11) Tsybeskov, L.; Hirschman, K. D.; Duttagupta, S. P.; Zacharias, M.; Fauchet, P. M.; McCaffrey, J. P.; Lockwood, D. J. Nanocrystalline-Silicon Superlattice Produced by Controlled Recrystallization. *Appl. Phys. Lett.* **1998**, *72*, 43−45.

(12) Zacharias, M.; Bläsing, J.; Veit, P.; Tsybeskov, L.; Hirschman, K.; Fauchet, P. M. Thermal Crystallization of Amorphous Si/SiO_2 Superlattices. *Appl. Phys. Lett.* **1999**, *74*, 2614−2616.

(13) Grom, G.; Lockwood, D.; McCaffrey, J.; Labbe, H.; Fauchet, P.; White, B.; Diener, J.; Kovalev, D.; Koch, F.; Tsybeskov, L. Ordering and Self-Organization in Nanocrystalline Silicon. *Nature* **2000**, *407*, 358−361.

(14) Navarro-Urrios, D.; Pitanti, A.; Daldosso, N.; Gourbilleau, F.; Rizk, R.; Garrido, B.; Pavesi, L. Energy Transfer between Amorphous Si Nanoclusters and Er^{3+} Ions in a SiO_2 Matrix. *Phys. Rev. B: Condens. Matter Mater. Phys.* **2009**, *79*, 193312.

(15) Pitanti, A.; Navarro-Urrios, D.; Prtljaga, N.; Daldosso, N.; Gourbilleau, F.; Rizk, R.; Garrido, B.; Pavesi, L. Energy Transfer Mechanism and Auger Effect in Er^{3+} Coupled Silicon Nanoparticle Samples. *J. Appl. Phys.* **2010**, *108*, 053518.

(16) Fu, Y. Light Emission and Slot Waveguide Effect in Er-doped SiO_2/Si Nanocrystalline Multilayer Structures. *Ph.D. Thesis*, University of Rochester, 2012.

DOI: 10.1021/acsphotonics.5b00515
ACS Photonics 2016, 3, 564−570

(17) AJA Sputtering System Brochure. http://goo.gl/z1aHFo (accessed 2014).
(18) Fu, Y.; Krzyzanowska, H.; Ni, K. S.; Fauchet, P. M. Suppression of Free Carrier Absorption in Silicon Using Multislot SiO_2/nc-Si Waveguides. *Opt. Lett.* **2013**, *38*, 4849−4851.
(19) Wojdak, M.; Klik, M.; Forcales, M.; Gusev, O. B.; Gregorkiewicz, T.; Pacifici, D.; Franzò, G.; Priolo, F.; Iacona, F. Sensitization of Er Luminescence by Si Nanoclusters. *Phys. Rev. B: Condens. Matter Mater. Phys.* **2004**, *69*, 233315.
(20) Pacifici, D. Erbium Doped Silicon Nanoclusters for Microphotonics. *Ph.D. Thesis*, University of Catania, 2003.
(21) Takeoka, S.; Fujii, M.; Hayashi, S. Size-Dependent Photoluminescence from Surface-Oxidized Si Nanocrystals in a Weak Confinement Regime. *Phys. Rev. B: Condens. Matter Mater. Phys.* **2000**, *62*, 16820−16825.
(22) Wolkin, M. V.; Jorne, J.; Fauchet, P. M.; Allan, G.; Delerue, C. Electronic States and Luminescence in Porous Silicon Quantum Dots: The Role of Oxygen. *Phys. Rev. Lett.* **1999**, *82*, 197−200.
(23) Bagolini, L.; Mattoni, A.; Fugallo, G.; Colombo, L.; Poliani, E.; Sanguinetti, S.; Grilli, E. Quantum Confinement by an Order-Disorder Boundary in Nanocrystalline Silicon. *Phys. Rev. Lett.* **2010**, *104*, 176803.
(24) Estes, M.; Moddel, G. Luminescence from Amorphous Silicon Nanostructures. *Phys. Rev. B: Condens. Matter Mater. Phys.* **1996**, *54*, 14633−14642.
(25) Wehrspohn, R. B.; Chazalviel, J. N.; Ozanam, F.; Solomon, I. Spatial versus Quantum Confinement in Porous Amorphous Silicon Nanostructures. *Eur. Phys. J. B* **1999**, *8*, 179−193.
(26) Allan, G.; Delerue, C.; Lannoo, M. Quantum Confinement in Amorphous Silicon Layers. *Appl. Phys. Lett.* **1997**, *71*, 1189−1191.
(27) Kanemitsu, Y.; Iiboshi, M.; Kushida, T. Photoluminescence Dynamics of Amorphous Si/SiO_2 Quantum Wells. *Appl. Phys. Lett.* **2000**, *76*, 2200−2202.
(28) Mott, N. F.; Davis, E. A. *Electronic Processes in Non-Crystalline Materials*; OUP: Oxford, 2012.
(29) Tsang, C.; Street, R. A. Recombination in Plasma-Deposited Amorphous Si:H. Luminescence Decay. *Phys. Rev. B: Condens. Matter Mater. Phys.* **1979**, *19*, 3027−3040.
(30) Stachowitz, R.; Schubert, M.; Fuhs, W. Nonradiative Recombination and Its Influence on the Lifetime Distribution in Amorphous Silicon. *Phys. Rev. B: Condens. Matter Mater. Phys.* **1995**, *52*, 10906.
(31) Delerue, C., Allan, G., Lannoo, M. In *Light Emission in Silicon: From Physics to Devices*; Lockwood, D., Ed.; Academic Press, 1997.
(32) Kanemitsu, Y.; Fukunishi, Y.; Kushida, T. Decay Dynamics of Visible Luminescence in Amorphous Silicon Nanoparticles. *Appl. Phys. Lett.* **2000**, *77*, 211−213.
(33) Allan, G.; Delerue, C.; Lannoo, M. Electronic Structure of Amorphous Silicon Nanoclusters. *Phys. Rev. Lett.* **1997**, *78*, 3161−3164.
(34) Dovrat, M.; Goshen, Y.; Jedrzejewski, J.; Balberg, I.; Sa'ar, A. Radiative versus Nonradiative Decay Processes in Silicon Nanocrystals Probed by Time-Resolved Photoluminescence Spectroscopy. *Phys. Rev. B: Condens. Matter Mater. Phys.* **2004**, *69*, 155311.
(35) Izeddin, I.; Timmerman, D.; Gregorkiewicz, T.; Moskalenko, A. S.; Prokofiev, A. A.; Yassievich, I. N.; Fujii, M. Energy Transfer in Er-doped SiO_2 Sensitized with Si Nanocrystals. *Phys. Rev. B: Condens. Matter Mater. Phys.* **2008**, *78*, 035327.
(36) Fujii, M. Coexistence of Two Different Energy Transfer Processes in SiO_2 Films Containing Si Nanocrystals and Er. *J. Appl. Phys.* **2004**, *95*, 272−280.
(37) Izeddin, I.; Moskalenko, A. S.; Yassievich, I. N.; Fujii, M.; Gregorkiewicz, T. Nanosecond Dynamics of the Near-Infrared Photoluminescence of Er-doped SiO_2 Sensitized with Si Nanocrystals. *Phys. Rev. Lett.* **2006**, *97*, 207401.
(38) Savchyn, O.; Ruhge, F.; Kik, P.; Todi, R.; Coffey, K.; Nukala, H.; Heinrich, H. Luminescence-Center-Mediated Excitation as the Dominant Er Sensitization Mechanism in Er-doped Silicon-Rich SiO_2 Films. *Phys. Rev. B: Condens. Matter Mater. Phys.* **2007**, *76*, 195419.
(39) Dunstan, D. J.; Boulitrop, F. Photoluminescence in Hydrogenated Amorphous Silicon. *Phys. Rev. B: Condens. Matter Mater. Phys.* **1984**, *30*, 5945−5957.
(40) Tsang, C.; Street, R. A. Luminescence Decay in Glow-Discharge Deposited Amorphous Silicon. *Philos. Mag. B* **1978**, *37*, 601−608.
(41) Dexter, D. L. A Theory of Sensitized Luminescence in Solids. *J. Chem. Phys.* **1953**, *21*, 836−850.
(42) Forster, T. 10th Spiers Memorial Lecture. Transfer Mechanisms of Electronic Excitation. *Discuss. Faraday Soc.* **1959**, *27*, 7−17.
(43) Lu, Y.-W.; Julsgaard, B.; Petersen, M. C.; Jensen, R. V. S.; Pedersen, T. G.; Pedersen, K.; Larsen, A. N. Erbium Diffusion in Silicon Dioxide. *Appl. Phys. Lett.* **2010**, *97*, 141903.
(44) Yoo, H. M.; Fu, Y.; Riley, D.; Shin, J. H.; Fauchet, P. M. Birefringence and Optical Power Confinement in Horizontal Multi-Slot Waveguides Made of Si and SiO_2. *Opt. Express* **2008**, *16*, 8623−8628.
(45) Press, W.; Teukolsky, S.; Vetterling, W.; Flannery, B.; Ziegel, E.; Press, W.; Flannery, B.; Teukolsky, S.; Vetterling, W. *Numerical Recipes in C*; Cambridge University Press, 1992.

DOI: 10.1021/acsphotonics.5b00515
ACS Photonics 2016, 3, 564−570